PCCP

PAPER

Performance of thermally-chargeable supercapacitors in different solvents

Cite this: *Phys. Chem. Chem. Phys.*, 2014, **16**, 12728

Received 14th April 2014,
Accepted 2nd May 2014

DOI: 10.1039/c4cp01610f

www.rsc.org/pccp

Hyuck Lim,[a] Cang Zhao[b] and Yu Qiao*[ab]

The influence of solvent on the temperature sensitivity of the electrode potential of thermally-chargeable supercapacitors (TCSs) is investigated. For large electrodes, the output voltage is positively correlated with the dielectric constant of solvent. When nanoporous carbon electrodes are used, different characteristics of system performance are observed, suggesting that possible size effects must be taken into consideration when the solvent molecules and solvated ions are confined in a nanoenvironment.

Low-grade heat (LGH) is one of the important energy sources that currently cannot be fully utilized.[1] An example of a LGH source is the waste heat in power generation plants, ranging about hundreds of giga-watt in the U.S. alone.[2] Other examples include geo-thermal energy, ocean thermal energy, distributed solar thermal energy, among others.[3] The low temperature makes LGH harvesting prohibitively difficult by using conventional thermal-to-electrical energy conversion (TEEC) techniques. The major issue for conventional indirect TEEC procedures is high installation, operational, and maintenance costs. The upper limit of the energetic efficiency is determined by the Carnot cycle: $\zeta_c = \Delta T/T$, where T is the LGH temperature and ΔT is the temperature difference. For a high-temperature heat source, the Carnot cycle limit is quite high, so that the overall TEEC efficiency $\zeta = \zeta_c \cdot \zeta_m$ may be sufficient, where ζ_m is the machine efficiency. For LGH, while the system costs may be similar, ζ considerably decreases, resulting in a poor cost-performance balance (~a few U.S. dollars per watt).[4] For direct, Seebeck-effect-based conventional TEEC procedures, the key challenges are associated with the low energy density and the poor energetic efficiency,[5] which is caused by both the low Carnot cycle limit and the thermal shorting effect.[6] As a result, the cost of the harvested power may be even much higher than that of the indirect procedures.

In a recent experiment,[7,8] we investigated the concept of thermally-chargeable supercapacitors (TCSs). As depicted in Fig. 1, a TCS consists of two half-capacitors at different temperatures. Each half-capacitor is formed by immersing an electrode in an electrolyte solution. At the electrode–liquid interface, solvated ions are adsorbed and an electrode potential is developed. When temperature changes, the adsorption coverage becomes different and the electrode potential varies. Thus, as the two half-capacitors are connected, a net output voltage is produced. This process can be greatly promoted if large-surface-area, nanostructured electrodes are employed. The preliminary testing data showed that TCSs work well for LGH. The energy density of a TCS can be on the scale of 10^2 mJ g^{-1}, with a relatively small ΔT of ~50 °C.

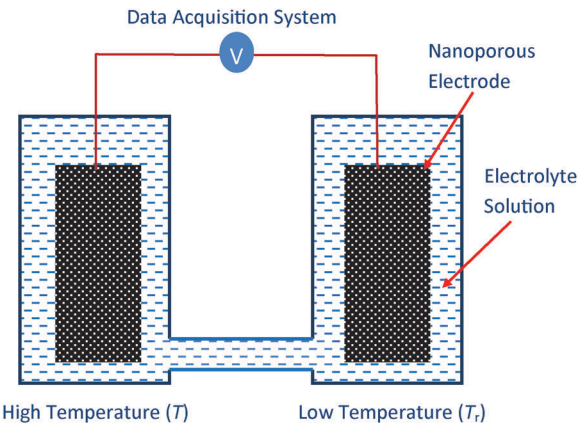

Fig. 1 Schematic of the experimental setup.

One of the key factors dominating the TCS performance is the output voltage, V. With a given ΔT, V is related to a number of factors, such as the electrode materials and the solvent properties. In the current study, we investigated three different solvents: dimethyl sulfoxide (DMSO), water, and formamide (FA); and two electrode materials: platinum (Pt) foil and nanoporous carbon (NC).

The Pt foil electrode was 100 μm thick, with the size of 10 mm × 10 mm. Two electrodes were separately placed in two polypropylene (PP) containers, each of which contained 50 ml of 1 M aqueous, DMSO, or FA solution of lithium chloride (LiCl). The containers were connected by a salt bridge, which was 5 mm in diameter and 30 mm long. The potential difference

[a] *Program of Materials Science & Engineering, University of California – San Diego, La Jolla, Ca 92093, USA. E-mail: yqiao@ucsd.edu*
[b] *Department of Structural Engineering, University of California – San Diego, La Jolla, CA 92093-0085, USA*

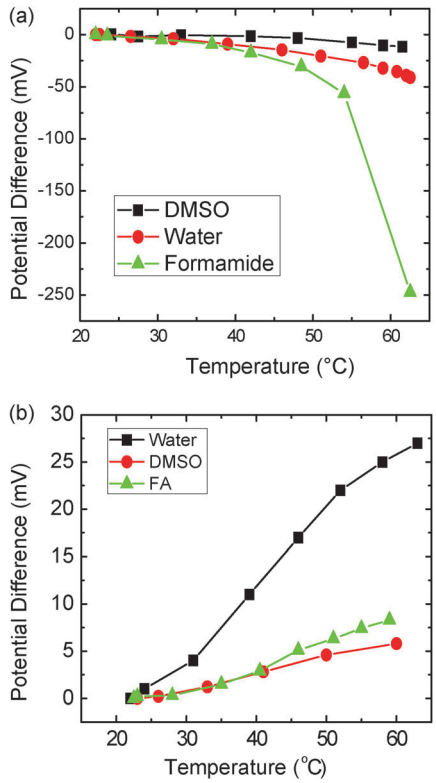

Fig. 2 Typical measurement results of the output voltage (V) as a function of the LGH temperature (T): (a) Pt electrodes and (b) nanoporous carbon electrodes.

between the two electrodes was measured using a National Instrument SCB-68 Data Acquisition (DAQ) system.

Initially, both containers were kept at room temperature, 23 °C. By using a Corning PC-220 Hot Plate, one of the containers was heated to 63 °C, with a constant rate of 3 °C min^{-1}. The temperature was recorded by using type-K thermocouples with an Omega HH-20A Reader. Fig. 2(a) shows the measured V. The average thermal sensitivity of electrode potential, dV/dT, is shown in Fig. 3.

The NC electrode material was obtained from Cabot (Product No.: BP2000). By using a Micromeritics TriStar-3000 Gas Adsorption Analyzer, the modal value of the pore size was determined to be ~3 nm. The specific surface area was 1810 m^2 g^{-1}. The particle size ranged from 1 to 50 μm. The material was refluxed in acetone at 80 °C for 4 h in a vertical tower, and filtered and repeatedly rinsed with warm water and methanol. By using a type 5580 Instron machine, about 200 mg of the treated NC particles were pressurized into a thin disk, with the diameter of around 5 mm. The NC-based TCS testing setup and procedure were similar to that of the Pt-based TCS.

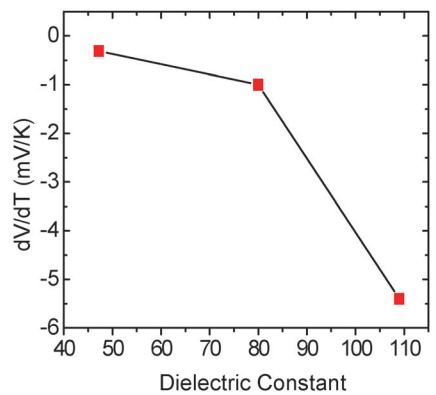

Fig. 3 The temperature sensitivity of electrode potential (dV/dT) as a function of the dielectric constant of the solvent. The data are for the Pt-electrode system.

As the electrode is immersed in the electrolyte solution, the effective surface ion density is much higher than that in the bulk liquid phase. As a result, counter charges are induced in the electrode surface, generating an electrode potential, ϕ. As temperature changes, due to the thermally dependent surface ion density and motion, the electrode potential would vary. Thus, as the two electrodes in a TCS are at different temperatures, a net output voltage, V, is measured. The associated electrical energy is harvested from the thermal energy.

The variation in the potential difference between the electrode and the bulk liquid phase can be stated as $\Delta\phi = \Delta(Q/C)$, where Q is the effective surface charge density and C is the effective surface capacitance, and "Δ" indicates the thermally induced change. In an electrolyte solution, a solid–liquid interface consists of a few capacitive components: C_M that captures the contribution of the electrode at the Jellium edge, C_H that reflects the solvent contribution in the Helmholtz layer, and C_{DL} that is related to the diffuse layer. The potential difference between the electrode phase and the bulk liquid phase can be written as $\Delta\phi = \Delta Q(1/\Delta C_M + 1/\Delta C_H + 1/\Delta C_{DL})$.[9] All the three terms are thermally dependent, among which C_M is related to only the electrode phase while C_H and C_{DL} are dependent on the solvent properties.[10] According to Trasatti,[11] the electrode potential at the potential of zero charge (PZC) state is related to the temperature variation. Under the PZC condition, the contributions from the charges in the electrode or the liquid are secondary. The thermal sensitivities of surface potential (dg^S_{dipole}/dT) are −1.15 mV °C^{-1}, −1.23 mV °C^{-1} and −1.66 mV °C^{-1} for DMSO, water, and FA, respectively. From Fig. 2(a) and 3, it can be seen that the average values of dV/dT are −5.4 mV °C^{-1}, −1.0 mV °C^{-1}, and −0.3 mV °C^{-1} for FA, water, and DMSO, respectively. The trend predicted by the Trasatti theory quantitatively fits with the experimental data, while is weaker. The difference between them may come from the influence of the adsorbed ions. Since the capacitance associated with specifically adsorbed ions (C_{ads}) is smaller compared with other capacitive components,[12] it has a dominant effect on the overall surface capacitance, C_{tot}. In a solution of a relatively high ion concentration, the degree of adsorption also tends to be high, as reported in ref. 13 that chlorine ions can generate a large potential difference. Under this condition, C_M and C_{ads} are smaller than C_H and C_D, and $\Delta\phi$ should be expressed as $\Delta\phi = \Delta Q(1/\Delta C_M + 1/\Delta C_{ads})$.

As the solvent is changed, the degree of adsorption becomes different. The adsorption process consists of three steps: removal of the solvation shell, removal of the solvent layer, and adsorption. There is a certain free energy change associated with each step, and the overall system free energy is lowered after the

adsorption process is completed. Usually, a solvent of a higher dielectric constant has a higher solvation ability. For the solvents under investigation, FA has the highest dielectric constant and DMSO has the lowest dielectric constant. Therefore, on the electrode surface, FA tends to have the lowest degree of adsorption and DMSO tends to have the highest degree of adsorption, causing the observed solvent effect on dV/dT.

While the classic theory explains well the data of Pt electrodes, according to Fig. 2(b), the solvent effects on the NC electrode based system are entirely different. For water, FA, and DMSO, the thermal sensitivity of output voltage is 0.68 mV $^{\circ}C^{-1}$, 0.23 mV $^{\circ}C^{-1}$, and 0.15 mV $^{\circ}C^{-1}$, respectively. First, the output voltage is positively correlated with temperature, T. Second, there is no clear pattern of the relationship between dV/dT and the dielectric constant of solvent. Both of the characteristics are contradictory to the above discussion, and should be related to the confinement effects of nanopore walls. In the NC electrode, the majority of the solid–liquid interface is in the smallest nanopores of the size ranging from 1 to a few nm. On such a small length scale, the solvated structure can be distorted, and, therefore, the free energy change associated with the removal of the hydration shell can be different from that at a large solid surface, and the influence of solvent molecules on the degree of adsorption varies. Furthermore, the surface ion structure is strongly affected by the nanopore surfaces, and the double layer structure may break down.[14] In the smallest nanopores, the confined liquid phase is exposed to the solid atoms, and the concept of the surface zone should be redefined [*e.g.* ref. 15]; somewhat similar phenomena have been reported for carbon-based supercapacitors.[16]

Probably most importantly, due to the ultrahigh surface to volume ratio, the liquid in the interior may not be regarded as a bulk phase, and the dominant ion motion is along the axial direction. Moreover, the molecular size of solvent becomes critical. The sizes of water, DMSO, and FA molecules are 0.25 nm, 0.47 nm, and 0.62 nm, respectively. Thus, as a first order approximation, the sizes of the solvated lithium cation are 0.65 nm, 1.09 nm, and 1.39 nm for the three solvents, respectively. While for water the smallest nanopores provide a barely enough space to form the Helmholtz layer, for DMSO and FA the space is insufficient. Consequently, the ion motion in DMSO and FA is suppressed, leading to the reduced thermal sensitivity.

In summary, it was confirmed experimentally that for a large electrode, conventional surface theory explains well the solvent effects on the output voltage of a TCS. However, when the electrodes are nanoporous, the conventional theory breaks down, which must be attributed to the confinement effects of nanopore walls. The details of the thermally driven nanofluidics behaviors are still under investigation.

Acknowledgements

This work was supported by the National Science Foundation under Grant No. ECCS-1028010.

References

1 A. Kapil, I. Bulatov, J. Kim and R. Smith, *Chem. Eng. Trans.*, 2010, **21**, 367.
2 R. H. Lasseter and P. Paigi, *Microgrid: A Conceptual Solution*, 35th Annul IEEE Power Electronics Specialists Conference, 2004.
3 D. Tanner, *Renewable Energy*, 1995, **6**(3), 367–373.
4 W. W. Husband and A. Beyene, *Int. J. Energy Res.*, 2008, **32**(15), 1373–1382.
5 M. S. Dresselhaus, G. Chen, M. Y. Tang, R. G. Yang, H. Lee, D. Z. Wang, Z. F. Ren, J. P. Fleurial and P. Gogna, *Mater. Res. Soc. Symp. Proc.*, 2006, **886**, 1–10.
6 G. S. Nolas and J. Sharp, *Thermoelectrics*, Springer, 2010.
7 Y. Qiao, V. K. Punyamurtual, A. Han and H. Lim, *J. Power Sources*, 2008, **183**(1), 403–405.
8 Y. Qiao, V. K. Punyamurtula and A. Han, *Appl. Phys. Lett.*, 2007, **91**, 153102.
9 J. O'M Bockris, A. K. N. Reddy and M. Gamboa-Aldeco, *Modern electrochemistry 2A-Fundamentals of Electrodics*, Kluwer Academic/Plenum Publishers, 2000, ch. 6.
10 W. R. Fawcett, *Liquids, Solutions and Interfaces*, Oxford University Press, 2004, ch. 10.
11 S. Trasatti, *Electrochim. Acta*, 1987, **32**(6), 843–850.
12 J. R. Macdonald and C. A. Barlow Jr, *J. Chem. Phys.*, 1962, **36**(11), 3062.
13 R. Payne, *Trans. Faraday Soc.*, 1968, **64**, 1638–1655.
14 K. Yang, T.-Y. Ying, S. Yiacoumi, C. Tsouris and E. S. Vittoratos, *Langmuir*, 2001, **17**, 1961.
15 K. Yang and S. Yiacoumi, *J. Chem. Phys.*, 2002, **117**(18), 8499.
16 J. Chmiola, G. Yushin, Y. Gogotsi, C. Portet, P. Simon and P. L. Taberna, *Science*, 2006, **313**, 1760.

